

Diffusion tensor imaging to assess gray and white matter microstructural brain abnormalities in a feline model of alpha-mannosidosis

Manoj Kumar¹, Jeff T Duda¹, Sea-Young Yoon², Jessica Bagel³, Patricia O'Donnell³, Charles Vite³, Stephen Pickup¹, James C Gee¹, John H Wolfe², and Harish Poptani¹

¹Radiology, University of Pennsylvania, Philadelphia, Pennsylvania, United States, ²Research Institute of the Children's Hospital of Philadelphia, Philadelphia, Pennsylvania, United States, ³School of Veterinary Medicine, University of Pennsylvania, Philadelphia, PA, United States, Pennsylvania, United States

Introduction: Alpha-mannosidosis (AMD) is an autosomal recessively inherited lysosomal storage disorder, which is caused by deficiency of the enzyme α -D-mannosidase. This enzyme is involved in the degradation of glycoproteins, thus its deficiency leads to accumulation of oligosaccharides in cells including that of the brain, kidney and liver¹. This rare and naturally occurring disease has been reported in humans² and has been replicated in cat³ and mouse⁴ models. AMD affected cats have similar clinical signs and pathology as seen in children with AMD. Abnormalities in the brain of AMD cats have been reported by single voxel MRS⁵ (increased oligosaccharides) as well as diffusion weighted MRI⁶ (decreased ADC). However no diffusion tensor imaging (DTI) studies have been reported in this model.

Materials and Methods:

Experimental Animals: Wild type and AMD affected cats were raised under NIH and USDA guidelines for the care and use of animals in research. Affected AMD cats were bred from carrier cats, and were genotyped for the mutant allele by PCR and restriction enzyme⁷. Physical and neurological examinations were performed weekly from birth up until the animals were euthanized. Animals were euthanized with an intravenous injection of euthasol. The cats were then transcardially perfused with cold saline. After perfusion fixation, the brains were removed and stored at 4°C in 4% paraformaldehyde (PFA) solution for 7 days to fix the brain tissue.

Ex vivo DTI: The ex vivo DTI were performed on Wild type controls (n=9) and AMD cats (n=5). Prior to imaging, brain samples were removed from the fixative and immersed in PBS for 48 hrs at 4°C. Brain sample was then placed in a plastic tube filled with proton-free susceptibility-matching fluid. DTI data were acquired on a Varian 9.4T horizontal bore magnet attached to a Varian Direct Drive console equipped with 20 G/cm gradients. A 70 mm i.d. transmit-receive quadrature birdcage coil (M2M, Cleveland, OH) was used for all studies. DTI was performed using a PGSE sequence modified to acquire 2D multi-slice images with diffusion weighting along 6 non-collinear directions optimally selected for anisotropy measurement. The b-value was set to 1027.36 s/mm²; TR=2.3s; TE=35.69ms; FOV=40x40mm², slice thickness=1mm, number of slices=51, number of averages=12, with matrix size=128x128 with total scan time is ~14 hrs/brain sample.

In vivo DTI: The in vivo DTI study was performed on AMD affected (n=3) and wild type (n=3) cats on 3T Tim Trio MRI (Siemens, Erlangen, Germany) equipped with a single-channel 11 cm i.d. transmit-receive birdcage coil (M2M, Cleveland, OH, USA). DTI images were acquired using a single shot spin echo EPI based sequence using 30 directions with following parameters: FOV=80 x100 mm², slice thickness=2 mm, number of slices=20, TR=3000 ms, TE=75 ms, Avg=8, b-values: 0 and 1000s/mm² with ~13min acquisition time. Physiological monitoring included pulse oximetry and vital signs (oxygen saturation and heart rate) were recorded before and during scanning.

Data processing and quantification: For ex vivo DTI data, image reconstruction from acquired FID files was performed using custom software routines in IDL and saved in the DTI studio format. A Gaussian filter (width 0.5) was used to smooth the data and reduce noise from the images. The Camino toolkit⁸ was used to reconstruct the diffusion tensors from the data set along with relevant scalar metrics such fractional anisotropy (FA) and mean diffusion (MDx10⁻⁶mm²/s). A template B0 image was created using the ANTs toolkit⁹ and each sample's B0 image. A threshold was chosen to create a brain segmentation template that excluded background signal. For each control sample, the FA image was thresholded at 0.2 and the resulting binary image was used as a set of seeds for whole-brain deterministic tractography using Camino. Each set of fibers was used to create an image of streamline density. These streamline density images were then warped into the template space, averaged, and normalized to create a probabilistic segmentation of the total white matter. A corresponding probabilistic gray matter mask was created by subtracting the white matter area from the brain segmentation (Fig. 1). In vivo DTI data processing and analysis were performed using DTI studio, version 3.0.2 was used to correct images for motion and eddy-current artifacts using a 12-mode affine transformation with automated image registration scheme.

ROI Analysis: FA and MD maps were generated from both ex vivo and ROI based analysis was performed separately. Bilateral ROIs were drawn on left and right side of the brain in each region except the corpus callosum (where a single ROI on the mid axial slice of the color coded brain map was drawn). Six gray and five white matter regions were chosen from the template image and individual ROI files were saved as image files to extract the FA and MD values from the individual data from both controls and affected samples (Fig 2). Similar ROIs were used for in vivo data using DTI studio. Independent Student's T-test was used to compare FA and MD values between AMD affected and control cats from ex vivo and in vivo data.

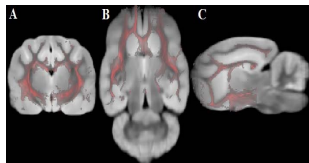


Fig. 1: Demonstrating segmentation of gray and white matter from whole brain. Pink color represents white matter while gray color represents gray matter.

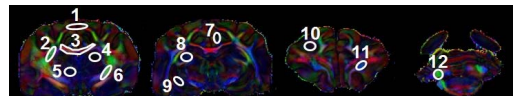


Fig. 2: Placement of bilateral ROIs in gray and white matter regions used for both ex vivo and in vivo DTI data analysis except in corpus callosum, where only a single ROI was used. 1=Cerebral cortex, 2=External capsule, 3=Corpus callosum, 4=Hippocampus, 5=Thalamus, 6=Internal capsule, 7=Cingulate gyrus, 8=Caudate nucleus, 9=Putamen, 10=Occipital cortex, 11=Corticospinal tract, 12=Cerebral peduncle.

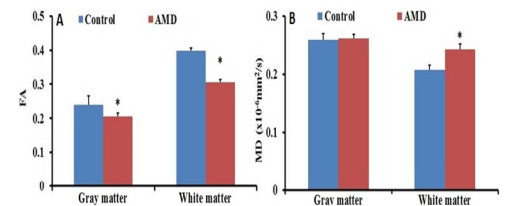


Fig. 3: Bar graph demonstrating FA and MD values from the ex vivo DTI studies of AMD and controls cat brains from gray and white matter of the brain. Asterisk (*) represents significant differences. (n<0.05).

Results: We observed significantly reduced FA from both gray (p=0.04) and white matter (p<0.001, Fig. 3A). We also observed significantly increased MD from white matter (p=0.02) in AMD cats compared to

controls. The MD values from the gray matter of AMD cats were not significantly higher than the controls (p=0.87) (Figure 3B). Significantly reduced FA was observed in all above mentioned white matter regions in AMD affected compared to control from in vivo DTI.

Discussion: Significantly reduced FA values in the white matter regions from both ex vivo and in vivo DTI may be due to increased gliosis or demyelination in the brains of AMD cats. Histological studies have reported increased gliosis, loss of axons, and myelin in the brain of AMD cats⁶. Previously Vite CH et al., reported significantly reduced gray and white matter ADC in AMD cats, while we saw an increase in ADC (MD) from ex vivo samples. A possible explanation for this discrepancy is that our data was collected from fixed brains in which variability in ADC measurements have been reported before⁶ while FA values are preserved¹⁰. The current study demonstrates that the abnormalities in diffusion anisotropy of the gray and white matter can be detected using DTI. As DTI is commonly performed in the clinic, these studies can further aid in clinical assessment of AMD and other LSDs and may eventually be used to monitor disease progression or response to therapy.

References: [1] Michalski JC, et al. Biochim Biophys Acta 1999; 1455:69-84. [2] Sung JH, et al. J Neuropathol Exp Neurol 1977;36:807-20. [3] Cummings JF, et al. J Vet Intern Med 1988;2:163-70. [4] Stinchi S, et al. Hum Mol Genet 1999;8:1365-72. [5] Magnitsky S, et al. NMR Biomed. 2010;23:74-9. [6] Vite CH, et al. AJNR 2008;29:308-13. [7] Berg T, et al. Biochem J 1997;328:863-870. [8] Cook PA, et al. ISMRM, 2006, p. 2759. [9] Bai J, et al. Magn Reson Imaging. 2012; 30:789-98. [10] Sun SW et al. Magn. Reson. Med., 2003; 50; 743-748. [11].

Acknowledgement: This study was funded by the NIH grants R01-DK063973 and Small Animal Imaging Facility (SAIF).